

Hydrothermal evolution of the Sar-Kuh porphyry copper deposit, Kerman, Iran: A fluid inclusion and sulfur isotope investigation

Soheila Nourali*, Hassan Mirnejad

Department of Geology, University College of Science, University of Tehran, Tehran, Iran

*Corresponding author, e-mail: s_nourali@yahoo.com

(received: 10/01/2012 ; accepted: 28/11/2012)

Abstract

Sar-Kuh porphyry copper deposit is located 6 km southwest of the Sar-Cheshmeh copper mine, Kerman Province, Iran. Based on field geology, petrography and fluid inclusions studies, four alteration types have been identified in the Sar-Kuh area. Early hydrothermal alteration formed a potassic zone in the central parts of Mamzar granite/grano-diorite stock and propylitic alteration in its peripheral parts. The late hydrothermal activity caused a limited phyllic and argillic alteration zones. The mineralized quartz veins are classified into four groups, on the basis of mineralogy and cross-cutting relationships. Group I and II veins are concentrated mainly in the potassic alteration zone, while group III and IV are most abundant in the phyllic and propylitic alteration zones, respectively. Fluid inclusion studies on group I and II quartz veins show that potassic alteration has originated from a dominantly magmatic fluid with high salinity (30-50 wt % NaCl equiv) and temperature ($>300^{\circ}\text{C}$). The $\delta^{34}\text{S}$ values of separated pyrite and chalcopyrite from samples range between +1.29‰ to +4.72‰ (mean value of +2.68‰), consistent with a magmatic origin for sulfur. Consequently, the meteoric water penetrated into peripheral and internal parts of stock along a network of late fractures mixed with magmatic water and produced a hydrothermal fluid with salinity ranging from 10 to 20 wt % NaCl equiv. This fluid produced propylitic as well as limited phyllic and argillic alterations in the peripheral of stock and volcanic rocks. Fluid inclusions are trapped at pressure of 300 to 3500 bar, but most of them are trapped at pressure of >1000 bar. The low grade of Cu (0.4 % Cu) and relatively high pressure of fluid entrapment at Sar-Kuh can be attributed to the emplacement of Mamzar stock at moderate to great depths. As the result of over-pressuring and thus low-density development of vein stockworks, the mineralizing fluids failed to provide sites for concentrating high grades of copper. Therefore, Sar-Kuh is considered a sub-economic porphyry copper deposit.

Keywords: Porphyry copper deposit, Hydrothermal alteration, Fluid inclusions, Sulfur isotopes, Sar-Kuh, Iran.

Introduction

Most porphyry copper deposits are the products of subduction-related magmatism and are commonly discovered in continental and oceanic arcs of Tertiary to Quaternary ages (Cooke *et al.*, 2005). These deposits from around the world and of all ages show similar patterns of vein and alteration distribution (Gustafson & Hunt, 1975; Beane & Bodnar, 1995; Sedorff *et al.*, 2005). The porphyry copper deposits in Iran occur dominantly in a region known as the Urumieh-Dokhtar magmatic belt that was formed due to the subduction of the Arabian plate beneath central Iran micro-continent during the Cenozoic Alpine orogeny (Berberian & King, 1981; Pourhosseini, 1981; Niazi & Asoudeh, 1978). This continental arc-style magmatism produced several porphyry deposits such as the Sungun porphyry copper-molybdenum deposit in northwest as well as the Sar-Cheshmeh porphyry copper deposit in southeast of Iran.

The Sar-Kuh porphyry copper deposit is located between the longitudes $55^{\circ}47'06''$ - $55^{\circ}49'45''$ and latitudes $29^{\circ}55'28''$ - $29^{\circ}57'05''$, 6 km southwestern of Sar-Cheshmeh mine. Sar-Kuh area is developed

in a mountainous terrain with elevations ranging from 2950 to 3100 m (Fig. 1). Despite extensive studies on alteration, fluid inclusions and isotopes in these porphyry copper deposits, no previous fluid inclusion and sulfur isotope data are available for smaller deposits such as Sar-Kuh. A regional exploration program was carried out by the Institute for Geological and Mining Exploration, Yugoslavia in 1972 that indicated Sar-Kuh as a target for detailed exploration activity. Factors such as the vicinity to the Sar-Cheshmeh mine and the possible use of the already established Cu smelting factories have justified mining exploitation at the Sar-Kuh area. For that reason, the National Iranian Copper Industries Company (NICICO) has recently drilled 12 exploration wells in Sar-Kuh and obtained more than 1400 m drill core samples from the hypogene alteration zone. In other investigations at Sarkuh, Barzegar (1993) made a study of petrography and alteration and then used statistical analysis for detection of alteration limits. Abbaslu (1999) showed the presence of four main alteration zones (potassic, phyllic, argillic and propylitic) and specified mineralization in different zones. Kan

Iran company presented a report on geological and alteration studied at Sarkuh deposit in 2008 and concluded that potassic alteration is the most common alteration type and introduced Sarkuh deposit as a porphyry system without Au and Mo elements. Fluid inclusions in vein quartz from porphyry Cu deposits trap fluids with a wide range of compositions under various pressure and temperature conditions. In a single deposit, hydrothermal fluids may originate from magmatic, sedimentary, or meteoric water sources (Bowman *et al.*, 1987; Dilles, 1987). It is suggested that sulfur isotope ratios may provide an additional aid whereby the economic geologist may be better equipped to learn more about the different sources of hydrothermal solutions and to obtain a better understanding about the processes by which hydrothermal mineral deposits have been formed. In this paper, we present the results of fluid inclusions and sulfur isotopes studies on the drill core samples with the purpose of understanding the source and evolution of hydrothermal fluids that formed porphyry Cu deposit in Sar-Kuh. It is also a goal of this study to investigate factors led to sub-economic Cu concentration in this deposit.



Figure 1: The Sar-Kuh area, Kerman, Iran.

Geological and Structural Setting

The main tectonic units of Iran are interpreted as the products of three major sequential geotectonic events: 1- subduction of the Neo-Tethyan oceanic plates beneath the Iranian lithospheric plate during Early to Late Cretaceous time, 2- obduction of Neo-Tethyan oceanic slivers (ophiolites) over the continental margin through Late Cretaceous time and 3- collision of The Arabian (Afro-Arabian) continental lithosphere with the Iranian plate during Late Cretaceous to Quaternary (Alavi, 1994; 2004). These geotectonic events developed three major

parallel structural units from west to central Iran, consisting of: I - The Zagros fold belt comprises 4 to 7 km thick Paleozoic and Mesozoic sediments which are overlain by Cenozoic carbonate and siliciclastic rocks with a thickness of 3 to 5 km. II- The Sanandaj-Sirjan zone consists of metamorphosed and nonmetamorphosed rocks as well as obducted ophiolites from the suture zone. III- The Urumieh-Dokhtar belt is formed by a subduction-related voluminous NW-SE trending magmatic arc which is separated from the Sanandaj-Sirjan metamorphic zone by the depressions of the Urumieh lake, Gavkhuni and Jazmurian lagoons (Fig. 2). Copper mineralization in Iran occurs dominantly within six structural-magmatic zones, including: Urumieh-Dokhtar, Western Alborz, Kavir-Sabzevar, Sabalan, Lut, and Makran. Among these, Urumieh-Dokhtar magmatic belt contains the largest number of porphyry copper mineralization. In central Iran, Cu mineralization is concentrated in several major porphyry Cu ore deposits and prospects in the Kerman Cenozoic magmatic assemblage, known as Kerman belt (Fig. 3). Most porphyry Cu mineralization in Kerman belt was coeval with or occurred after the emplacement of mid-late Miocene granitoids (Shafiei, 2008). The length of the Kerman belt is approximately 450 km long with an average width of 80 km. A number of major porphyry copper deposits occurs in the Kerman belt including: Sar-Cheshmeh deposit, that contains 1200 million tons of sulfide ore with an average grade of 0.64 % Cu and ~0.03 % Mo (Waterman & Hamilton, 1975) and Miduk deposit containing 125 million tons of sulfide ore with 0.82 % Cu (Taghipour *et al.*, 2008). The other important porphyry copper deposits that occur in Kerman belt are Chah Firuzeh which contains Cu sulfide grading >1 % (Hezarkhani, 2009) and Darreh Zar that contains 0.64 % Cu (Nedimovic, 1973).

The oldest rock types exposed in Sar-Kuh are Eocene tuffs, andesite, andesite-basalt and pyroclastic breccias, intruded by an E-W trending Oligocene Mamzar stock consisting of a granodiorite core and a granite rim. Intrusion of Mamzar stock into the Eocene volcanic rocks has created a contact metamorphic aureole consisting of hornfels facies rocks. The Sar-Kuh porphyry copper deposit is hosted by granite/grano-diorite stock. Mamzar stock is also cut, particularly in its central parts, by Miocene micro quartz diorite porphyry dykes

which are responsible for mineralization, alteration and construction of porphyry system in the area of

Sar-Kuh (Fig. 4).

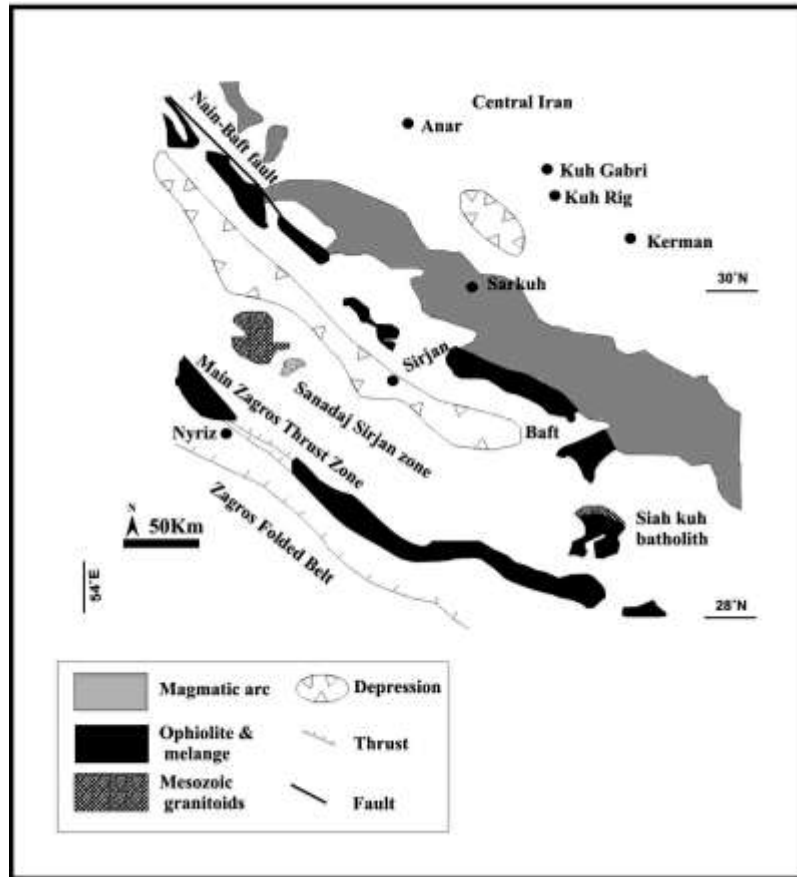


Figure 2: Simplified structural map of central Iran (Stöcklin & Nabavi, 1973; Berberian, 1981b; Shahabpour, 2005).

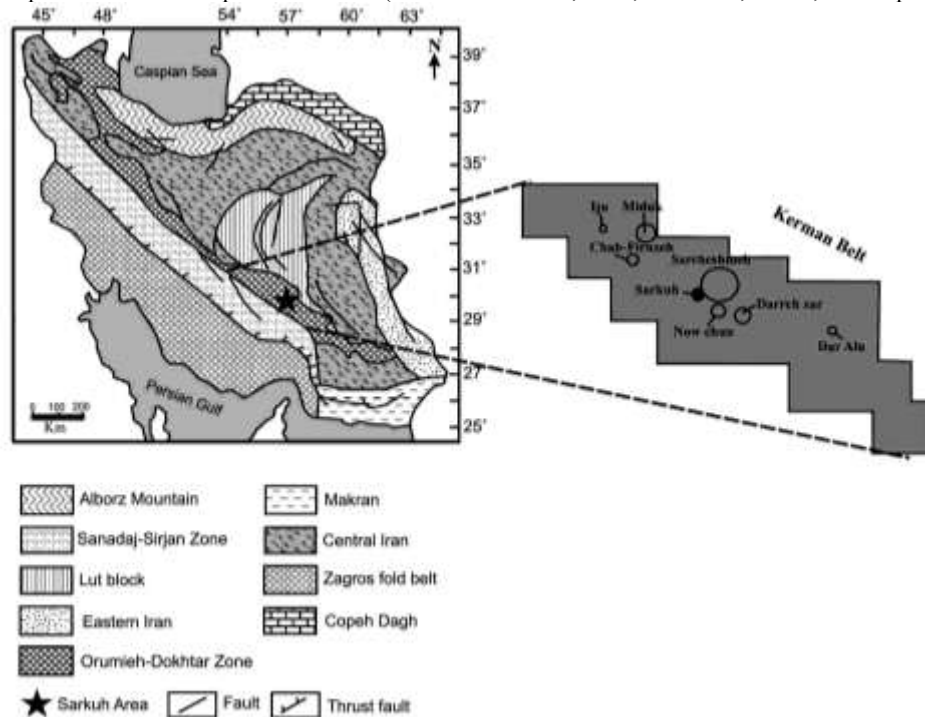


Figure 3: Geological map of Iran (modified from Stöcklin, 1977; Shahabpour, 1994) and the location of Sar-Kuh with respect to major porphyry copper deposits and prospect in the Kerman copper belt.

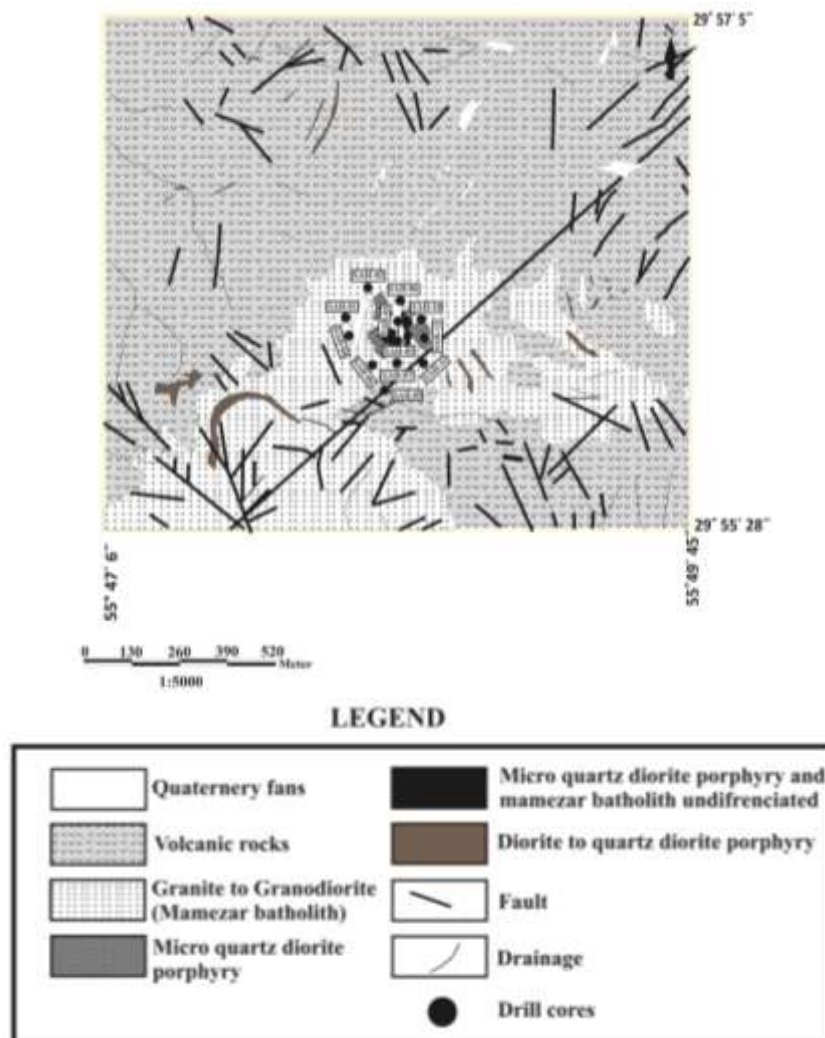


Figure 4: Simplified geologic map of Sar-Kuh area (Kan Iran, 2008).

Analytical Methods

For this study, a number of samples were collected from drill holes and outcrops at Sar-Kuh deposit. A total of 75 thin sections, 23 polished-thin sections and 4 doubly polished-thin sections were prepared for petrography and fluid inclusions studies. Total of 98 thin and polished sections were examined under transmitted and reflected light at the geology department of Tehran University, Tehran, Iran. Micro-thermometric studies were carried out on doubly polished-thin sections. Temperatures of phase changes in fluid inclusions were measured using a Fluid Inc. Linkam-type gas-flow stage at Kan-Azin laboratory, Tehran. This instrument operates by passing precooled N_2 gas around the sample. Stage calibration was performed using synthetic fluid inclusions. Accuracy at standard reference temperatures was $\pm 0.2^\circ C$ at $-56.6^\circ C$ (triple point of CO_2), $\pm 0.1^\circ C$ at $0^\circ C$ (melting point

of ice), $\pm 2^\circ C$ at $374.1^\circ C$ (critical homogenization of H_2O), and $\pm 9^\circ C$ at $573^\circ C$ (alpha to beta quartz transition). The heating rate was approximately $1^\circ C/min$ near the temperatures of phase transitions. Sulfur isotope analyses were performed on 11 pure pyrite and chalcopyrite grains, collected from hypogene zone. Powder of sulfide minerals with approximately twice the amount of tungsten oxide (WO_3) were weighted in to tin capsules and then flamed at $1800^\circ C$, using the VarioEL III Elemental Analyzer. Isotope ratios were measured on a Finnigan-MAT 252 multi-collector mass spectrometer at the Hatch stable isotope laboratory, University of Ottawa, Ontario, Canada.

Hydrothermal Alteration and Mineralization

Hydrothermal alteration and mineralization at Sar-Kuh are centered on the Mamzar granite/granodiorite batholith. Based on petrography and

mineralogy of collected samples, four main hypogene alteration zones are found in the Sar-Kuh porphyry copper deposit: potassic, phyllic, argillic and propylitic. Early hydrothermal alteration was dominantly of potassic and propylitic nature, which was later followed by phyllic and argillic alterations. In addition to these, intermediate

hydrothermal alteration zones such as potassic – argillic or potassic – phyllic as well as accessory silicic alteration are found. To show the position of alteration zones and the variation of Cu grade in different alteration zones with depth, two cross sections were drawn through the exploration drill holes (Fig. 5).

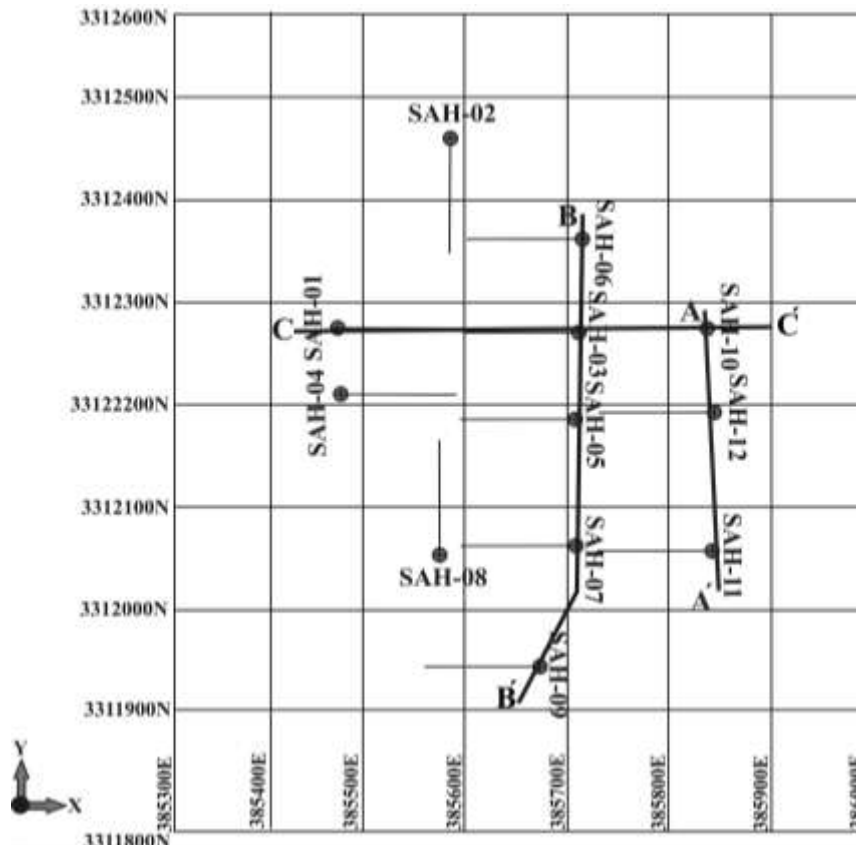


Figure 5: The position of exploration drill holes in Sar-Kuh area. Two cross-sections (A-A' and B-B') were selected to investigate the variation of Cu concentration with depth and alteration type (see figure 4).

In general, potassic zone has a relatively large extension but phyllic zone has a limited distribution at Sar-Kuh. Another observation is that the copper grade reaches the highest in the potassic alteration and decreases toward other alteration zones such as phyllic and transition alteration zones (Fig. 6). The drill cores that are located at the center of the Sar-Kuh area and vicinity of micro quartz diorite porphyry have characteristically higher grades of copper.

Potassic alteration

The earliest and most common alteration in the Sar-Kuh porphyry copper deposit is represented by potassic mineral assemblage that has been developed in the deep and central parts of the Sar-

Kuh intrusive. The potassic zone in the Sar-Kuh porphyry copper deposit consists of quartz + K-feldspar + biotite + plagioclase + sericite (Fig. 7a). Also, microcline and chlorite are occasionally observed in this alteration zone. Opaque minerals consist of chalcopyrite, pyrite, molybdenite, magnetite and hematite. The main Cu bearing ore is chalcopyrite, and occurs as dissemination, vein, open space filling and veinlets within quartz veins. Petrographic observations indicate the presence of two distinct types of biotite within this alteration zone: 1. Primary biotite, which is brown in color and generally euhedral, 2. Hydrothermal biotite, which is mainly pale-brown to greenish-brown in color and anhedral. Potassic alteration displays a close spatial association with Cu mineralization.

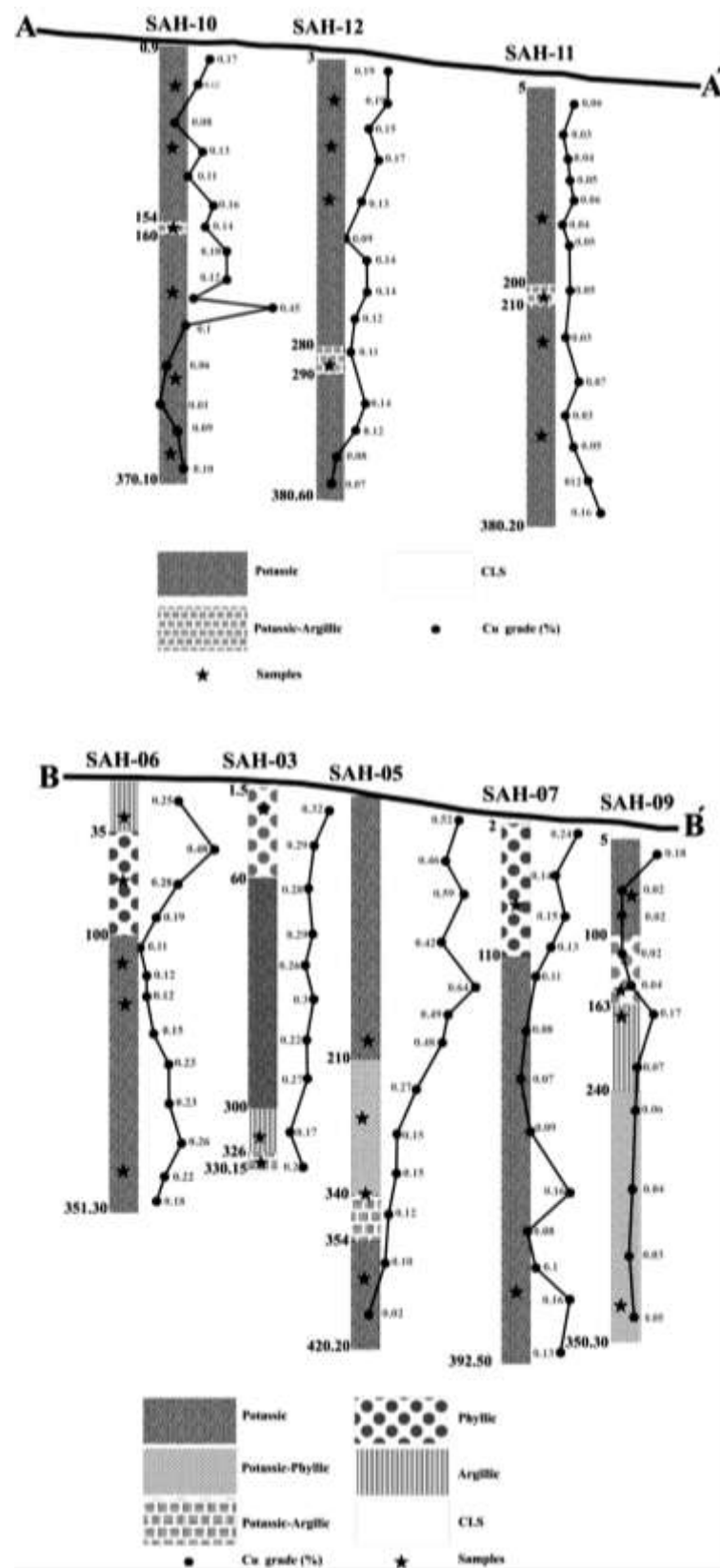


Figure 6: The profiles along A-A' and B-B' sections that illustrate the variations of Cu grade with depth and hypogene alteration type.

Propylitic alteration

Propylitic alteration consists of calcite + chlorite +

epidote + sericite + actinolite + pyrite (Fig. 7b) and is common in the peripherals and particularly in the

SE part of the stock, as well as in the surrounding volcanic rocks. Propylitic alteration is represented by chloritization of primary and secondary biotite, and epidotization of plagioclase. Locally, plagioclase is replaced by clays and sericite. Phenocrysts of amphibole are partly altered to

chlorite. Within the zone of transition, both potassic and propylitic alteration minerals are found along side each other, specified by hydrothermal biotite, K-feldspar, chlorite and/or epidote mineral assemblages.

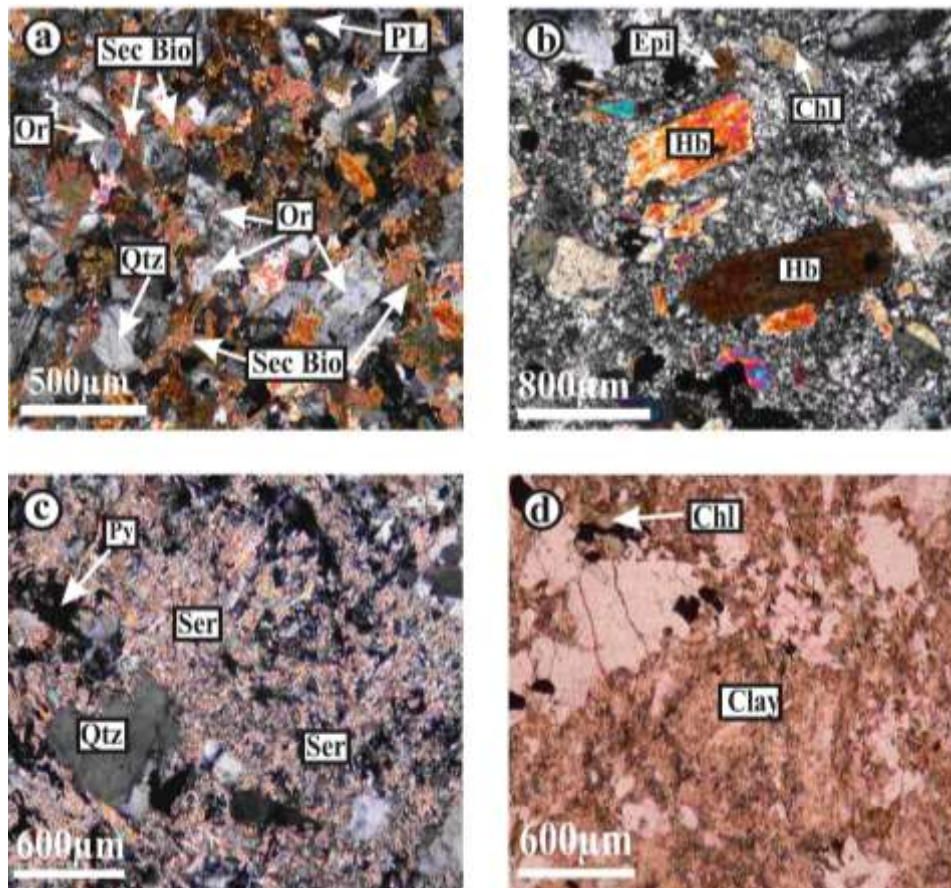


Figure 7: Photomicrograph of (a) potassic alteration, (b) propylitic alteration, (c) argillic alteration, (d) phyllic alteration that affected Mamzar batholith in Sar-Kuh area. Plain polarized light. Or = Orthoclase, Qtz = Quartz, Sec Bio = Secondary Biotite, Epi = Epidote, Chl = Chlorite, Hb = Hornblende, Py = Pyrite.

Argillic alteration

Argillic alteration occurs around the potassic alteration zone within the granite and grano-diorite as well as in the surrounding volcanic and pyroclastic rocks. This type of alteration consists of clay minerals such as kaolinite, montmorillonite, illite, pyrophyllite as well as goethite, jarosite, hematite, sericite, chlorite and quartz (Fig. 7c). Clay minerals have been produced from alteration of K-feldspar. The affected rocks are soft and white, but can change to brown color by increasing in the amount of iron-oxides.

Phyllic alteration

Phyllic alteration is formed by the leaching of

sodium, calcium and magnesium from aluminosilicates-bearing rocks. During this alteration, almost all rock-forming silicates were replaced by sericite and quartz (Fig. 7d). The transition from potassic to phyllic alteration is gradual and marked by an increase in the proportion of muscovite. Drilling cores and field studies show that phyllic alteration in Sar-Kuh has a limited extension. There is almost a transition zone between potassic and phyllic alterations, known as potassic-phyllic. Mineral assemblages in the potassic-phyllic alteration consist of quartz + K-feldspar + plagioclase + chlorite + sericite + muscovite + sulfide. Plagioclase and secondary K-feldspar, altered to sericite and biotite, are replaced

by chlorite.

Quartz vein classification

The stockwork system at Sar-Kuh deposit is developed mainly in the potassic zone and its peripheral parts. On the basis of mineralogy and cross-cutting relationships, it is possible to distinguish four main groups of veins.

Group I veins which are surrounded by potassic, and less commonly phyllic and propylitic alteration haloes. These veins consist of quartz + K-feldspar + pyrite + chalcocopyrite \pm molybdenite (Fig. 8a). Quartz comprises 70 to 95% volume of the veins.

Group II veins generally cross-cut, and in places off-set group I veins. These veins consist of quartz + pyrite + chalcocopyrite \pm bornite (Fig. 8b). Sulfide minerals are located mainly in a narrow discontinuous layer in the vein center, but in some

cases the sulfides are disseminated through the quartz. Group II veins occur in all alteration zones, but are concentrated mainly in the potassic alteration zone. In some cases, group II veins seem to have been formed as the result of the re-opening of group I veins.

Group III veins cross-cut both groups I and II veins and in some cases off-set the earlier-formed veins. Group III veins consist of quartz + calcite + pyrite \pm chalcocopyrite (Fig. 8c) and are most abundant in phyllic alteration zone.

Group IV veins cross-cut all the other vein groups and represent the youngest vein-forming event in the Sar-Kuh stock. These veins consist of quartz + calcite (Fig. 8d). Group IV veins are found mainly in the propylitic zone, but also occur locally in the phyllic and potassic alteration zones.

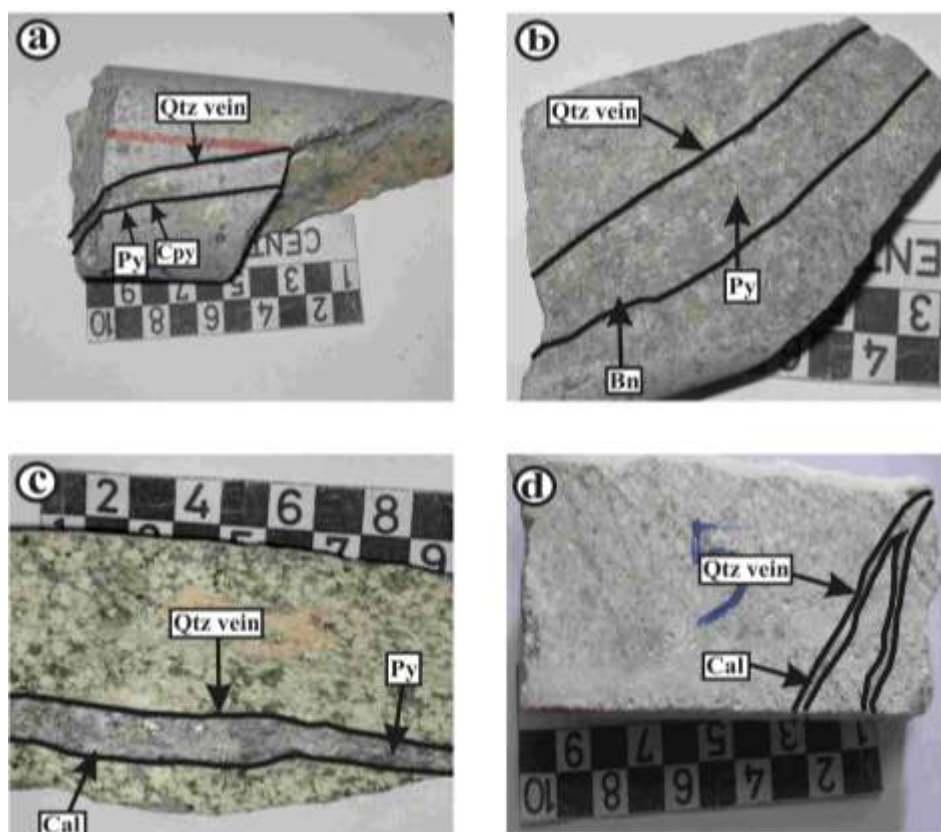


Figure 8. Classification of quartz veins in Sar-Kuh porphyry copper deposit. (a) Group I quartz (Qtz) vein with pyrite (Py) and chalcocopyrite (Cpy) grains, (b) Group II quartz vein with pyrite and bornite (Bn), (c) Group III quartz vein with pyrite and calcite (Cal), (d) Group IV quartz vein with calcite.

Fluid Inclusion Petrography and Microthermometry

Fluid Inclusion Petrography

Previous investigations of fluid inclusions in numerous porphyry copper deposits have shown a

complex variation in fluid temperature and composition in time and space (e.g., Eastoe, 1978; Preece & Beane, 1982; Reynolds & Beane, 1985) and Sar-Kuh is no exception. Samples examined for fluid inclusion study are representative of the

different vein and quartz stages described above and include I, II, III quartz veins. Fluid inclusions are abundant in the Sar-Kuh quartz veins and range from 1 up to 12 μm in diameter. Petrography of fluid inclusions illustrates the presence of primary, secondary and pseudo-secondary inclusions in the studied samples.

On the basis of abundance, nature and proportion of phases at room temperature, the studied fluid inclusions at Sar-Kuh deposit are classified into three main types. Liquid-vapor (LV) inclusions consist of liquid + vapor \pm solid phases. In this type of fluid inclusions, liquid phase is volumetrically dominant and vapor bubbles constitute 5-30% of the volume (Fig. 9a). The diameter of these fluid inclusions range between 2 to 12 μm . Vapor-liquid (VL) inclusions consist of vapor + liquid \pm solid

phases. Vapor bubbles comprise >70% of the inclusion volume, while liquid occupies less than 20% of the volume (Fig. 9b). In a small number of LV fluid inclusions, cubes of halite or opaque minerals occur (Fig. 9c). Liquid-vapor-halite-solid (LVHS) inclusions consist of liquid + vapor + halite + solid phases other than halite (Fig. 9d). Solid phases consist of sylvite, erythro-siderite and opaque minerals (e.g., hematite and chalcocopyrite). Halite was identified by their cubic and sub-cubic shapes and optical isotropy. Sylvite was distinguished from halite by its rounded edges and lower relief. Halite crystals are generally larger and more common than those of sylvite, and have a well-defined habit. Erythro-siderite was identified by its rounded shape, transparent to pale green color and strong birefringence.

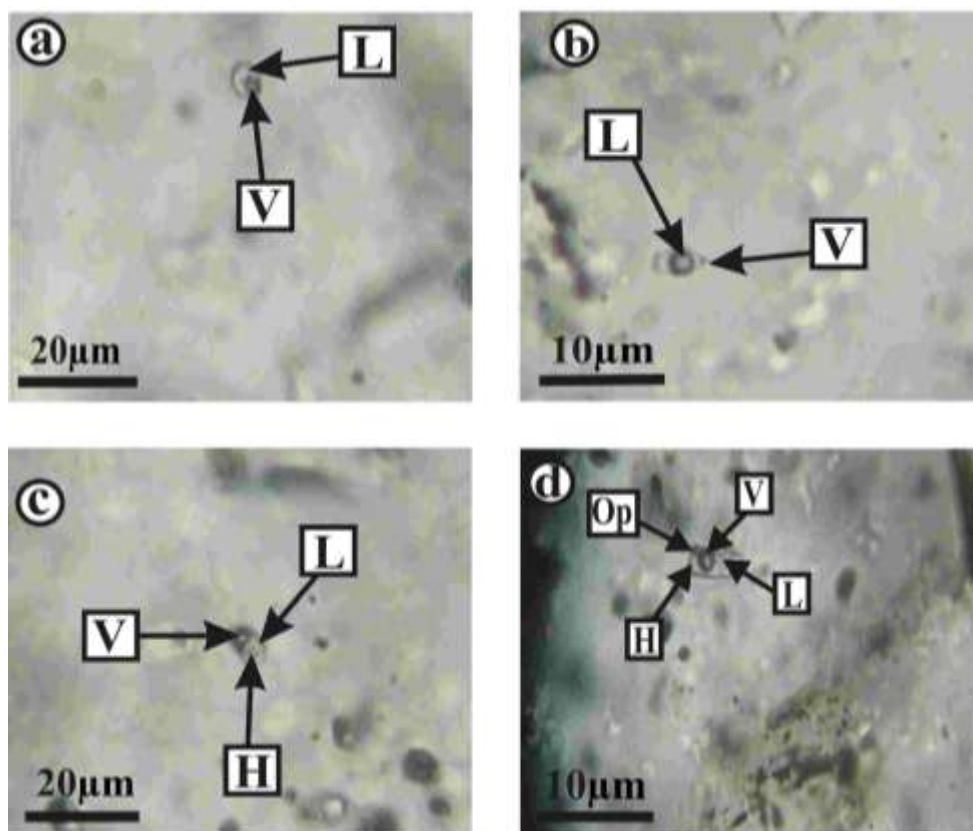


Figure 9: Photomicrograph of fluid inclusions from mineralized quartz veins at Sar-Kuh porphyry copper deposits. (a) LV (liquid+vapor), (b) VL (vapor + liquid), (c) LV associated with halite (liquid+vapor+halite), (d) LVHS (liquid + vapor + halite + solid).

Chalcocopyrite was identified on the basis of its optical characteristics such as opacity and triangular cross section. Hematite was easily identified by its red color, hexagonal shape, extremely high index of refraction and high birefringence.

Fluid Inclusion Microthermometry

Microthermometric studies were carried out on a number of quartz grains from group I, II and III veins (Table 1). Group IV veins did not contain workable fluid inclusions and were thus ignored during the measurements. Fluid inclusions were

analyzed by cycles of freezing down to $-160\text{ }^{\circ}\text{C}$ and heating up to $+600\text{ }^{\circ}\text{C}$. These cycles were generally repeated several times in order to avoid problems of the nucleation during freezing runs. The temperatures of initial (T_e) and final melting of ice ($T_{m_{ice}}$) were measured on types LV and LVHS fluid inclusions. In type VL inclusions, T_e was difficult to determine because of the high vapor/liquid ratios. The temperature of first ice melting (T_e) on most LV fluid inclusions was between -14.8 and $-55.7\text{ }^{\circ}\text{C}$ (Fig. 10a), suggesting that NaCl + KCl and CaCl_2 , FeCl_2 , MgCl_2 are the principal salts in solution. The $T_{m_{ice}}$ values for these inclusions range from -9.5 to $-33.2\text{ }^{\circ}\text{C}$ (Fig. 10b), corresponding to salinities of 13.4 to 39.7 wt % NaCl equiv, respectively (Sterner *et al.*, 1988) (Fig. 10c). LVHS type fluid inclusions are characterized by T_e values varying from -28.1 to

$-47.5\text{ }^{\circ}\text{C}$ (Fig. 10a). These eutectic temperatures normally suggest the presence of significant Fe and Mg in addition to Na and K (Sterner *et al.*, 1988). Eutectic temperatures for the $\text{CaCl}_2\text{-H}_2\text{O}$, $\text{NaCl-CaCl}_2\text{-H}_2\text{O}$, and $\text{FeCl}_3\text{-H}_2\text{O}$ systems are -45.1 , -53 and $-55\text{ }^{\circ}\text{C}$, respectively (Linke, 1965), and could explain the low first ice melting temperatures observed for some of the LVHS inclusions. The $T_{m_{ice}}$ values for LVHS inclusions range from -11 to $-17.7\text{ }^{\circ}\text{C}$ (Fig. 10b). The homogenization temperature of LV and LVHS fluid inclusions range from 173.1 to $406.1\text{ }^{\circ}\text{C}$ and 137.4 to $439.8\text{ }^{\circ}\text{C}$, respectively (Fig. 10d). Salinities of LVHS fluid inclusions based on the halite dissolution temperature range from 31 to 50.3 wt % NaCl equiv (Sterner *et al.*, 1988) (Fig. 10c). The halite dissolution temperatures for LVHS inclusions are 302.6 to $425.7\text{ }^{\circ}\text{C}$.

Table 1. Fluid inclusion microthermometric data from Sar-Kuh porphyry copper deposit, Kerman, Iran.

| Sample | Type | Size (um) | Phases | V- vapor (%) | V- liquid (%) | T_e ($^{\circ}\text{C}$) | $T_{m_{ice}}$ ($^{\circ}\text{C}$) | Th-v ($^{\circ}\text{C}$) | Th - S ($^{\circ}\text{C}$) | Th - S2 ($^{\circ}\text{C}$) | Th - S3 ($^{\circ}\text{C}$) | Salinity | Density |
|--------|------|-----------|-----------------|--------------|---------------|------------------------------|--------------------------------------|-----------------------------|-------------------------------|--------------------------------|--------------------------------|----------|---------|
| SAH-01 | P | 7 | V+L+S+S2+SO+SO2 | 10 | 60 | - | - | 137.4 | 302.6 | 310.4 | | 38.3641 | 1.2270 |
| SAH-02 | P | 6 | V+L | 50 | 50 | -14.8 | -9.5 | 406.1 | | | | 13.4077 | 0.7000 |
| SAH-03 | P | 12 | V+L+S | 25 | 60 | - | - | 193.7 | 325.1 | 398.1 | | 40.1927 | 1.2058 |
| SAH-04 | P | 8 | V+L+S+SO | 15 | 70 | - | - | 253.2 | 320.0 | | | 39.7643 | 1.1512 |
| SAH-05 | P | 8 | V+L+S+SO | 30 | 40 | - | - | 336.0 | 392.3 | | | 46.6142 | 1.1444 |
| SAH-06 | P | 8 | V+L+S+SO | 25 | 70 | - | - | 301.9 | 310.8 | | | 39.0123 | 1.0966 |
| SAH-07 | P | 8 | V+L+S+S2+SO | 25 | 60 | -28.1 | -19.3 | 332.2 | 287.7 | 421.2 | | 37.2385 | 1.0482 |
| SAH-08 | P | 8 | V+L+S+SO | 25 | 70 | - | - | 158.9 | 177.0 | | | 30.7866 | 1.1479 |
| SAH-09 | P | 7 | V+S+S2+L+SO+SO2 | 20 | 70 | -33.4 | -11.0 | 301.0 | 95.1 | 425.7 | | 50.3411 | 1.2228 |
| SAH-10 | P | 7 | V+L+S+SO | 25 | 30 | -31.1 | -14.7 | 344.5 | 313.7 | | | 39.2565 | 1.0558 |
| SAH-11 | P | 4 | V+L+S+SO | 30 | | -33.5 | -17.7 | 317.6 | 353.6 | | | 42.7386 | 1.1198 |
| SAH-12 | P | 7 | V+L+S+S2 | 25 | 25 | -36.2 | -14.6 | 439.8 | 321.3 | 341.7 | | 39.8728 | 0.9644 |
| SAH-13 | P | 10 | V+L | 30 | 70 | -32.9 | -12.8 | 319.4 | | | | 16.7036 | 0.8641 |
| SAH-14 | P | 6 | V+L | 10 | 90 | -37.9 | -12.2 | 230.7 | | | | 16.1454 | 0.9597 |
| SAH-15 | PS | 3 | V+L | 10 | 90 | -55.7 | -11.4 | 183.1 | | | | 15.3744 | 1.0003 |
| SAH-16 | P | 8 | V+S+L | 10 | 80 | - | -15.7 | 173.3 | 371.1 | | | 44.4313 | 1.2594 |
| SAH-17 | P | 8 | V+S+L+S2+SO | 20 | 70 | - | - | 211.9 | 346.7 | 371.6 | | 42.0983 | 1.2101 |
| SAH-18 | P | 4 | V+S+L | 10 | 85 | -39.4 | -33.2 | 242.3 | 320.1 | | | 39.7727 | 1.1612 |
| SAH-19 | P | 8 | V+L | 25 | 75 | -36.4 | -10.9 | 350.4 | | | | 14.8761 | 0.8037 |
| SAH-20 | P | 7 | V+S+L+S2+S2+SO | 20 | 60 | -39.2 | -11.0 | 224.5 | 187.2 | 278.8 | 414.7 | 31.2539 | 1.0965 |
| SAH-21 | P | 5 | V+S+L | 10 | 85 | -39.4 | -10.7 | 263.9 | 336.5 | | | 41.1799 | 1.1557 |
| SAH-22 | P | 10 | V+S+L+SO | 20 | 75 | -43.9 | -14.7 | 214.9 | 317.6 | | | 39.5656 | 1.1829 |
| SAH-23 | P | 6 | V+S+L+S2 | 10 | 80 | -47.5 | - | 170.2 | 234.0 | 324.7 | | 40.1588 | 1.2223 |
| SAH-24 | PS | 5 | V+S+L | 10 | 90 | -35.1 | -14.6 | 182.1 | 280.4 | | | 36.7113 | 1.1824 |

P = primary, Ps = pseudo-secondary, V = vapor, L = liquid, S = Solid, S₂ = second solid, SO = opaque solid, SO₂ = second opaque solid, T_e = eutectic temperature, $T_{m_{ice}}$ = ice melting temperature, Th = homogenization temperature.

Minimum temperature and pressure of fluid entrapment

Halite dissolution method ($T_{h(H)} > T_{h(V)}$) was used for the calculation of minimum pressure of fluid entrapment at the Sar-Kuh porphyry system. Pressure estimates were based on the intersection of fluid inclusion isochors with liquidus. Calculations show that fluid inclusions were

trapped at pressure of 300 to 3500 bars, but most of them were trapped at pressure of >1000 bar. This pressure corresponds to the depth of more over than 4 km. Minimum temperature of entrapment range from 300 to $400\text{ }^{\circ}\text{C}$ (Fig. 11).

Sulfur Isotope

In the Sar-Kuh Porphyry copper deposit, sulfur

isotope composition was studied on pyrite – chalcopyrite pair in quartz veins from potassic and phyllic alteration zones. The $\delta^{34}\text{S}$ values for sulfide minerals Sar-Kuh vary from +1.29 to +4.72‰, with an average value of +2.68‰ (Table 2). The $\delta^{34}\text{S}$ values of pyrite from potassic and phyllic alteration range from +2.39 to +3.03‰ and +2.67 to +3.26‰, respectively. The variation of $\delta^{34}\text{S}$ values for chalcopyrite from potassic and phyllic alterations

are +1.94 to +3.03‰ and +1.29 to +4.72‰, respectively. Sar-Kuh isotopic temperatures have been determined from the $\delta^{34}\text{S}$ values and the experimental fractionation curve for pyrite-chalcopyrite (Kajiwara and Krouse, 1971). This temperature range from 204 to 241.4°C and 565 to 657°C for sulfides collected from the phyllic and potassic alterations.

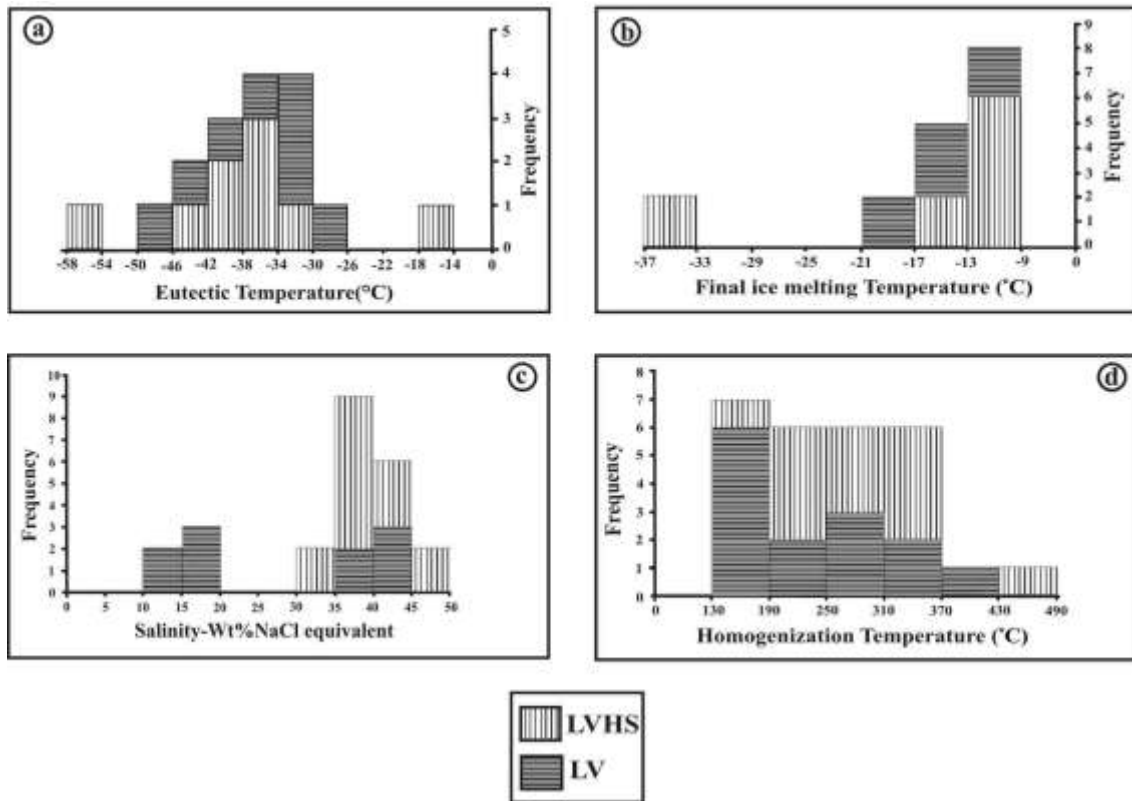


Figure 10: Histograms for LV and LVHS fluid inclusions from mineralized quartz veins at Sar-Kuh deposit. (a) Eutectic temperature, (b) Final ice melting temperature, (c) Salinity, (d) Homogenization temperature.

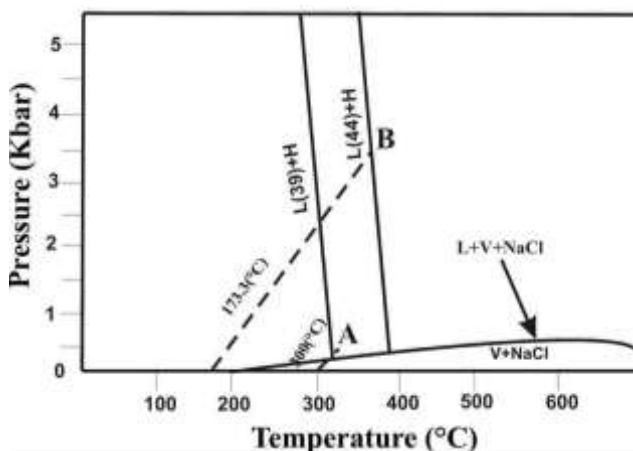


Figure 11: Temperature-pressure diagram of part of the NaCl-H₂O system (Bodnar, 1994). The dashed lines represent constant liquid-vapor homogenization temperatures which

extend from the L+V+H curve at 173.3 and 300. The $T_{h_{max}}=300$ and $T_{h_{min}}=173.3$ intersect the [L(39)+H] (point A) and [L(44)+H] (point B) liquidus, respectively. The range of these intersections for all data is between 0.3 Kbar (point A) and 3500 Kbar (point B). The L+V+H curve, slope of the T_h lines and liquidus lines are from Bodnar (1994).

Discussion

Fluid inclusion studies illustrate the presence of two different types of hydrothermal fluids at Sar-Kuh porphyry copper deposit. The earliest hydrothermal fluid with high salinity (30 to 50 wt % NaCl equiv) and high temperature (> 300°C) had a magmatic origin. This ortho-magmatic fluid moved upward to shallower levels, and its temperature subsequently decreased.

The progressive cooling of the ortho-magmatic

fluid is interpreted to stabilized K-feldspar and biotite at the expense of plagioclase and hornblende, respectively. This process led to potassic alteration in the central part of the intrusion. The ortho-magmatic fluid was also responsible for creating group I and II quartz veins. The presence of chalcopyrite in LVHS fluid inclusions and the association of the high salinity fluids with mineralized veins indicate that this early high temperature fluid transported Cu, Fe and S and eventually deposited chalcopyrite, bornite and pyrite at relatively low temperature (<300°C).

The meteoric water circulated in the peripheral parts of stock and portion of this water moved toward the center of the stock and after interaction with magmatic water, the magmatic fluid gradient decreased and then produced a mixture of magmatic and meteoric fluid with salinity of 10 to 20 wt % NaCl equiv. This fluid caused propylitic alteration in peripheral parts of stock and volcanic wall rocks and also produced argillic alteration partly. The fluid inclusion samples have been drawn on a scatter diagram (Fig. 12).

Table 2. Sulfur isotope compositions of pyrite and chalcopyrite from Sar-Kuh porphyry copper deposit, Kerman, Iran.

| Sample | Mineral | Deep (m) | Alt. zone | $\delta^{34}\text{S}$ |
|-----------|---------|----------|-----------|-----------------------|
| SAH-1-3 | Py | 134.60 | POT | +3.03 |
| SAH-1-3 | Cpy | 134.60 | POT | +2.46 |
| SAH-6-111 | Py | 357.50 | POT | +2.46 |
| SAH-6-111 | Cpy | 357.50 | POT | +1.94 |
| SAH-9-75 | Py | 349.50 | POT | +2.39 |
| SAH-9-75 | Cpy | 349.50 | POT | +3.03 |
| SAH-7-102 | Py | 38.5 | PHY | +3.26 |
| SAH-7-102 | Cpy | 38.5 | PHY | +1.29 |
| SAH-4-62 | Py | 230 | PHY | +2.8 |
| SAH-4-62 | Cpy | 230 | PHY | +4.72 |
| SAH-8-110 | Py | 212.60 | PHY | +2.67 |

Py= Pyrite, Cpy= Chalcopyrite, Alt. Zone= Alteration zone, POT= Potassic alteration, PHY= Phyllic alteration.

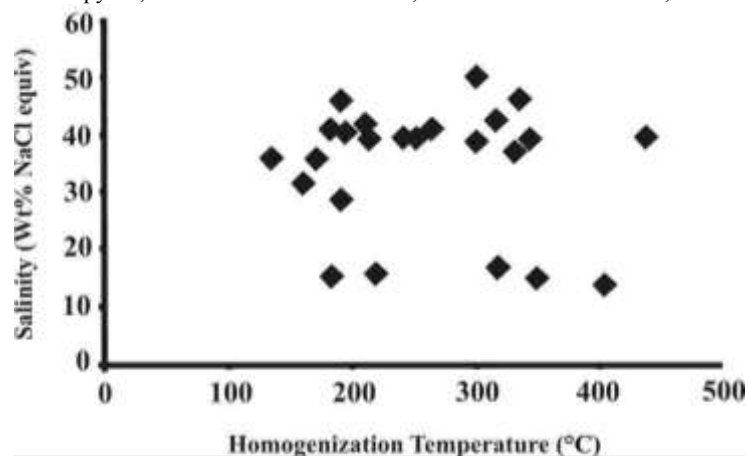


Figure 12: Scatter diagram for fluid inclusion samples.

Late fractures or reopened veins provided pathways for this fluid to circulate in the system. This fluid, when circulated in the central parts of the intrusion, progressively increased in temperature, causing destabilization of the previously formed K-feldspar from the potassic alteration and produced phyllic alteration zone, and leached away early formed copper sulfide minerals to upper levels of system

and precipitated limited proportion of chalcopyrite and bornite in some of the shallower parts of the phyllic alteration zone. In the study area, phyllic alteration, compared to other hydrothermal alteration types, has developed only locally. Low extension of phyllic alteration is probably due to the low quantity of meteoric water. The minimum pressures of fluid entrapment at Sar-Kuh porphyry

system has been estimated 300 to 3500 bars, but most of the fluid inclusions show pressure of >1000 bar (Fig. 11). Based on the estimated pressures of fluid inclusions, it is suggested that the depth of Mamzar stock emplacement at Sar-Kuh has been over than 4 km. The depth of emplacement at Sar-Kuh deposit is deeper than that of the other porphyry copper deposits in Uromieh - Dokhtar belt such as the Miduk (2.51 km, McInnes *et al.*, 2005), Sungun (2 km, Hezarkhani & Williams Jones, 1998) and Sar-Cheshmeh (4.75 km, McInnes *et al.*, 2005). At the same time, the concentration of copper in Sar-Kuh is lower (~ 0.4 %) relative to that in other porphyry copper deposits such as Sar-Cheshmeh (0.64 %, Waterman & Hamilton, 1975), Miduk (0.82 %, Taghipour *et al.*, 2008) and Sungun (0.76 %, Tabatabaei, 2002). The differences in Cu concentrations can be attributed to the deeper level emplacement of Mamzar stock and lower content of water in the magma, both of which can result in the limited distribution of stockwork system at Sar-Kuh porphyry system. A lack of extensive stockwork system normally causes the mineralizing fluids not to have enough open spaces for circulation and thus not being able to move to the distal areas for mineralization. Also, the deep emplacement of the Mamzar stock would have reduced the efficiency of copper extraction, by lowering the partition coefficient for Cu between the melt and aqueous phase (Shinohara *et al.*, 1984; Webster, 1995).

Based on fluid inclusion studies, the minimum temperature of fluid entrapment at Sar-Kuh is about 300 to 400°C (Fig. 11). The Sar-Kuh fluid inclusion data compared with Moonta deposit in South Australia (Ruano *et al.*, 2002), illustrate a similarity in salinity of fluid in both deposits and a difference between the minimum temperature of fluid entrapment is that fluid at Moonta deposit has entrapped at higher temperature than that of Sar-Kuh deposit. The presence of low eutectic temperature inclusions in both porphyry deposits suggest that these deposits formed from a similar composition fluid (poly-saline and multi-cation fluid). The fluid inclusion data from Sar-Cheshmeh deposit in Iran (Hezarkhani, 2006) illustrate that homogenization temperature and salinity of fluid at Sar-Cheshmeh is higher than that of Sar-Kuh.

Potassic alteration at Sar-Kuh porphyry copper deposit has an extensive development, which points to the effect of predominant magmatic hydrothermal fluid. According to Ohmoto & Rye

(1979), the $\delta^{34}\text{S}$ values for magmatic sulfides are $0 \pm 2\%$. The $\delta^{34}\text{S}$ values of sulfide minerals at Sar-Kuh suggest sulfur either deposited directly from magmatic fluid or was derived by dissolution and leaching of sulfide minerals in igneous rocks. Results of fluid inclusion micro-thermometry analysis also illustrate that dominant fluid at Sar-Kuh deposit is magmatic fluid. The lack of sulfate minerals in almost all veins and veinlets, where the sulfides are present, suggest that the ore-bearing fluids during sulfide mineralization had relatively low $f\text{O}_2$ (Ohmoto, 1986; Hoefs, 2009). Low abundance of magnetite at potassic zone of Sar-Kuh porphyry copper deposit also confirms low $f\text{O}_2$ of mineralizing fluid.

Temperatures calculated by sulfur isotope compositions of pyrite - chalcopyrite pairs are 204 to 657°C and those obtained by fluid inclusion micro-thermometry are 300 to 400°C. The overlap of two temperature ranges indicate that pyrite and chalcopyrite, while precipitating from hydrothermal solutions, were in isotopic equilibrium. On textural evidence, it seems clear that these sulfide phases were co-precipitated at Sar-Kuh deposit. The intergrowth of pyrite and chalcopyrite and inclusions of these minerals in quartz grains also point to isotopic equilibrium.

A sulfur isotope study on Panguna porphyry copper deposit in New Guinea has been carried out by Eastoe (1983). The sulfur isotopic composition of sulfide minerals in Panguna ranges from -1.4 to +3.1‰. The sulfur source has been interpreted to be magmatic. Isotopically, the sulfide minerals from Panguna are lighter than those of Sar-Kuh. Shelton & Rye (1982) summarized the sulfur isotope data at Mines Gaspé in Quebec. The $\delta^{34}\text{S}$ values of sulfide minerals in all veins except from IV veins, ranging from -3.9 to +1.1‰, are lighter than those at the Sar-Kuh deposit. The agreement of isotopic depositional temperature and fluid inclusion temperature from anhydrite bearing veins at Mines Gaspé illustrate that similar to Sar-Kuh, pyrite and chalcopyrite are in equilibrium conditions.

At Sungun porphyry copper deposit in Iran, Calagari (2003) indicated that $\delta^{34}\text{S}$ values of sulfide minerals fall in range from -4.6 to -0.3‰. These values are lighter compared to Sar-Kuh ones. In addition, pyrite and chalcopyrite minerals are not in isotopic equilibrium at Sungun deposit.

Conclusions

Based on petrography and mineralogy of drill cores and outcrop samples, four hydrothermal alteration types are recognized at Sar-Kuh: potassic; phyllic; argilic; propylitic. Fluid inclusion studies show the presence of two hydrothermal fluids at Sar-Kuh deposit. The fluid I, originated from high temperature and pressure magma, was the source of potassic alteration. This fluid is responsible for potassic alteration and Cu ± Mo mineralization. The fluid II, is a mixture of magmatic fluid with meteoric water which has low temperature and salinity, was responsible for propylitic alteration in the peripheral parts of porphyry system and volcanic wall rocks. This fluid produced limited phyllic alteration, because of low quantity and low injection of meteoric water in to the inner parts of system. The $\delta^{34}\text{S}$ values of sulfide

minerals at Sar-Kuh ranging from +1.29 to +4.72‰ that suggest a predominant magmatic origin for sulfur. The low grade of copper and high pressure of fluid entrapment points to a medium to high depth of stock emplacement. The low extension of stockworks system indicates limited circulation of fluids in the Sar-Kuh porphyry. All of these factors led Sar-Kuh deposit to become a sub-economic ore deposit.

Acknowledgements

The authors acknowledge National Iranian Copper Industries Company for allowing access to samples, maps and geochemical data. We would also like to thank Ms. Moghaddam for assistance with fluid inclusion microthermometry. The help by Hatch stable isotope laboratory in measuring sulfur isotope ratio is appreciated.

References

- Abbaslu, Z., 1999. Alteration halos studies at Sarkuh copper deposit. MSc thesis, Shahid Bahonar University of Kerman, Kerman.
- Alavi, M., 1994. Tectonic of the Zagros orogenic belt of Iran, new data and interpretations. *Tectonophysics*, 229: 211-238.
- Alavi, M., 2004. Regional stratigraphy of the Zagros fold-thrust belt of Iran and its proforeland evolution. *American journal of science* 304: 1-20.
- Barzegar, H., 1993. Economic geology studies at Sarkuh porphyry copper deposit. Msc thesis, Shahid beheshti university, Tehran.
- Bean, R.E., Bodnar, R.J., 1995. Hydrothermal fluids and hydrothermal alteration in porphyry copper deposits. In: Pierce, F.W., and Bohm, J.G. (Eds), *Porphyry copper deposits of the American Cordillera*, Arizona Geological Society Digest 20, Tuscon, AZ: 235-269.
- Berberian, M., 1981b. Generalized tectonic map of Iran, 1:6450000, Geological survey of Iran.
- Berberian, M., King, G.C., 1981. Toward a paleogeography and tectonic evolution of Iran. *Canadian Journal of Earth Sciences*, 18: 210-265.
- Bowman, J.R., Parry, W.T., Kropp, W.P., Kruer, S.A., 1987. Chemical and isotopic evolution of hydrothermal solutions at Bingham, Utah. *Economic Geology* 82: 395-428.
- Calagari, A.A., 2003. Stable isotope (S, O, H and C) studies of the phyllic and potassic alteration zones of the porphyry copper deposit at Sungun, East Azarbaijan, Iran. *Journal of Asian Earth Sciences* 21: 767-780.
- Cooke, D.R., Hollings, P., Walshe, J.L., 2005. Giant deposits characteristic, distribution and tectonic controls. *Economic Geology*, 100: 801-818.
- Dilles, J.H., 1987. Petrology of the Yerington batholith, Nevada: Evidence for evolution of porphyry copper ore fluids. *Economic Geology* 82: 1750-1789.
- Eastoe, C.J., 1978. A fluid inclusion study of the Panguna porphyry copper deposit, Bougainville, Papua New Guinea: *Economic Geology*, 73: 721-748.
- Eastoe, C.J., 1983, Sulfur isotope data and the nature of the hydrothermal systems at the Panguna and Frieda porphyry copper deposits, Papua New Guinea. *Economic Geology*, 78: 201-213.
- Gustafson, L.B., Hunt, J.P., 1975. The porphyry copper deposit at El Salvador, Chile. *Economic Geology*, 70: 857-912.
- Hezarkhani, A., Williams-Jones, A.E., 1998. Controls of alteration and mineralization in the Sungun porphyry copper deposit, Iran: Evidence from fluid inclusions and stable isotopes. *Economic Geology*, 93: 651-670.
- Hezarkhani, A., 2006. Hydrothermal evolution at the Sar-Cheshmeh porphyry Cu-Mo deposit, Iran: Evidence from fluid inclusion. *Journal of Asian Earth Sciences*, 28: 408-422.
- Hezarkhani, A., 2009. Hydrothermal fluid geochemistry at the Chah-Firuzeh porphyry copper deposit, Iran: Evidence from fluid inclusions. *Journal of Geochemical Exploration*, 101: 54-264.
- Hoefs, J., 2009. *Stable isotope geochemistry*. 6nd ed., Springer-Verlag Berlin, 293
- Kajiwara, Y., Krause, H.R., 1971. Sulfur isotope partitioning in metallic sulfide systems. *Canadian Journal. Earth Society*, 8: 1397-1408.

- Kan Iran exploration consulting engineers, 2008. Report on geological and alteration studies at Sar-kuh (1:5000), Tehran, Iran, National Iranian Copper Industries Company.
- Linke, W.F., 1965. Solubilities of inorganic and metal organic compound, II. Fourth symposium: American Chemical Society, Washington, DC, 73-79.
- McInnes, B.I.A., Evans, N.J., Fu, F.Q., Garwin, S., 2005. Application of thermo-chronology to hydrothermal ore deposits. *Rev. Mineral. Geochem.* 58: 467-498.
- Nedimovic, R., 1973, Exploration for ore deposits in Kerman region., Geological Survey of Iran, Rep 53, 247.
- Niazi, M., Asoudeh, I., 1978. The depth of seismicity in the Kermanshah region of the Zagros Mountains (Iran). *Earth and Planetary Science Letters*, 40: 270-274.
- Ohmoto, H., Rye, R.O., 1979. Isotopes of sulfur and carbon. In: Barnes, H.L. (Eds), *Geochemistry of hydrothermal ore deposits*. Wiley, New York, 509-567.
- Ohmoto, H., 1986. Stable isotope geochemistry of ore deposits. In: Valley, J.W., Taylor, H.P., and O'Neil, J.R. (Eds.), *Stable isotopes in high temperature geological processes*. Mineralogical Society of America, 16: 491-570.
- Omajev, V., 1972. Report on exploration at Sar-Kuh copper mineral occurrence, Beograd, Yugoslavia, Institute for Geological and Mining Exploration.
- Pourhosseini, F., 1981. Petrogenesis of Iranian plutons: A study of the Natans and Bazman intrusive complexes, Unpubl. Ph.D. thesis, University of Cambridge.
- Preece, R.K., Bean, R.E., 1982. Contrasting evolutions of hydrothermal alteration in quartz monzonite and quartz diorite wall rocks at the Sierrita porphyry copper deposit, Arizona. *Economic Geology*, 77: 1621-1641.
- Reynolds, T.J., Bean, R.E., 1985. Evolution of hydrothermal fluid characteristics at the Santa Rita, New Mexico, porphyry copper deposit. *Economic Geology*, 80: 1328-1347.
- Ruano, S.M., Both, R.A., Golding, S.D., 2002. A fluid inclusion and stable isotope study of the Moonta copper-gold deposits, South Australia: evidence for fluid immiscibility in a magmatic hydrothermal system. *Chemical Geology* 192: 211-226.
- Seedorf, E., Dilles, J. H., Proffett, J. M., Einaudi, M. T., Zurcher, L., Stavast, W. J. A., Johnson, D. A., Barton, M. D., 2005. Porphyry deposits: characteristics and origin of hypogene features. *Economic Geology* 100th Anniversary, 251-298.
- Shafiei, B., 2008. Metallogenic model of Kerman porphyry copper belt and it's exploratory approaches. Unpubl. Ph.D. thesis, Shaheed Bahonar University of Kerman, Iran.
- Shahabpour, J., 1994. Post-mineralization breccias dike from the Sar-Cheshmeh porphyry copper deposit, Kerman, Iran. *Exploration and Mining Geology*, 3: 39-43.
- Shahabpour, J., 2005. Tectonic evolution of the orogenic belt in the region located between Kerman and Neyriz. *Journal of Asian Earth Science*, 24: 405-417.
- Shelton, K.L., Rye, D.M., 1982. Sulfur isotopic compositions of ores from Mines Gaspé, Quebec: An example of sulfate-sulfide isotopic disequilibria in ore-forming fluids with application to other porphyry-type deposits. *Economic Geology*, 82: 1688-1709.
- Shinohara, H., Iiyama, J.T., Matsuo, S., 1984. Behavior of chlorine in the system granitic magma-hydrothermal solution. *Academie des Sciences de Paris: Comptes Rendus, Serie II* 298: 741-743.
- Sterner, S. M., Hall, D. L., Bodnar, R. j., 1988. Synthetic fluid inclusions. V. solubility of the system NaCl-KCl-H₂O under vapor-saturated conditions. *Geochimica et Cosmochimica*, 55: 989-1005.
- Stöcklin, J., Nabavi, M.H., 1973. Tectonic map of Iran, 1:250000, Geological survey of Iran.
- Stöcklin, J., 1977. Structural correlation of the Alpine range between Iran central Asia. *Memoire Hors-Serve No.8 dela Societe Geologique de France*, 8: 333-353.
- Tabatabaei, D., 2002. Geochemical investigation on the exploration significance of the lithochemical haloes at the Sungun porphyry (Cu-Mo)-skarn (Cu-Ag-Au), Ahar, Azerbaijan. MSc thesis, Shahid Bahonar University of Kerman, Kerman.
- Taghipour, N., Aftabi, A., Mathuer, R., 2008. Geology and Re-Os geochronology of mineralization of the Miduk porphyry copper deposit, Iran. *Journal Compilation*, 58: 143-160.
- Waterman, G.C., Hamilton, R.L., 1975. The Sar-Cheshmeh porphyry copper system. *Economic Geology*, 70: 568-576.
- Webster, J.D., 1995. Exsolution of Cl-bearing fluids from chlorine-enriched mineralizing granitic magmas and implications for ore metal transport: Prococeedings, Giant Ore Deposit II Conference, Queens University, Kingston, Ontario, Canada, 221-261.